σ_g = core-to-core Kihara distance parameter for a gas molecule at which distance the binary potential is 0, pm

σ_g^* = center-to-center Kihara distance parameter for a gas molecule = $\sigma_g + a_g$

σ_w = core-to-core Kihara distance parameter for a lattice water molecule at which distance the binary potential is 0, pm

σ = core-to-core distance parameter for interaction between a gas molecule and a lattice water molecule, pm

ω = acentric factor

LITERATURE CITED

American Petroleum Institute, *Technical Data Book—Petroleum Refining*, New York (1980.

Davidson, D. W., and J. A. Ripmeester, "Clathrate Ices—Recent Results," *J. Glaciology*, **21** (85) 33, (1978).

Dharmawardhana, P. B., W. R. Parrish, and E. D. Sloan, "Experimental Thermodynamic Parameters for the Prediction of Natural Gas Hydrate Dissociation Conditions," *Ind. Eng. Chem. Fund.*, **19** (4), 228 (1980).

Falabella, B. J., and J. Vanpee, "Experimental Determination of Gas Hydrate Equilibrium below the Ice Point," *Ind. Eng. Chem. Fund.*, **13** (3), 228 (1974).

Holder, G. D., and J. H. Hand, "Multiple-Phase Equilbria in Hydrates from Methane, Ethane, Propane and Water Mixtures," *AIChE J.*, **28** (3), 440 (1982).

Holder, G. D., and G. C. Grigoriou, "Hydrate Dissociation Pressures of (Methane + Ethane + Water). Existence of a Locus of Minimum Pressures," *J. Chem. Thermo.*, **12**, 1,093 (1980).

Holder, G. D., and S. Godbole, "Measurements and Prediction of Dissociation Pressures of Isobutane and Propane Hydrates below the Ice Point," *AIChE J.*, **28**, 930 (1982).

Holder, G. D., G. Corbin, and K. Papadopoulos, "Thermodynamic and Molecular Properties of Gas Hydrates from Mixtures Containing Methane, Argon, and Krypton," *Ind. Eng. Chem. Fund.*, **19** (3), 282 (1980).

Holder, G. D., and D. J. Manganiello, "Hydrate Dissociation Pressure Minima in Multicomponent Systems," *Chem. Eng. Sci.*, **37** (1), 9 (1982).

John, V. T., and G. D. Holder, "Choice of Cell Size in the Cell Theory of Hydrate Phase Gas-Water Interactions," *J. Phys. Chem.*, **85** (13), 1811 (1981).

John, V. T., and G. D. Holder, "Contribution of Second and Subsequent Water Shells to the Potential Energy of Guest-Host Interactions in Clathrate Hydrates," *J. Phys. Chem.* **86**, 455 (1982a).

John, V. T., and G. D. Holder, "Hydrates of Methane + n-Butane below the Ice Point," *J. Chem. & Eng. Data*, **27**, 18 (1982b).

Marshall, D. R., S. Saito, and R. Kobayashi, "Hydrates at High Pressures. I: Methane-Water, Argon-Water, and Nitrogen-Water Systems," *AIChE J.*, **10** (2), 202 (1964).

McLeod, H. O., Jr., and J. M. Campbell, "Natural Gas Hydrates at Pressures to 10,000 psia," *Trans. AIME*, **222**, 590 (1961).

Ng, H-J., and D. B. Robinson, "The Role of n-Butane in Hydrate Formation," *AIChE J.*, **22**, (4), 656 (1976a).

———, "The Measurement and Prediction of Hydrate Formation in Liquid Hydrocarbon-Water Systems," *Ind. Eng. Chem. Fund.*, **15**, (4), 293 (1976b).

Parrish, W. R., and J. M. Prausnitz, "Dissociation Pressures of Gas Hydrates Formed by Gas Mixtures," *Ind. Eng. Chem. Proc. Des. Dev.*, **11** (1), 26 (1972).

Robinson, D. B., and B. R. Mehta, "Hydrates in the Propane, Carbon Dioxide, Water System," *J. Can. Pet. Tech.*, **10** (1), 33 (1971).

Robinson, D. B., and J. M. Hutton, "Hydrate Formation in Systems Containing Methane, Hydrogen Sulfide and Carbon Dioxide," *J. Can. Pet. Tech.*, **I**, 1 (1967).

Rouher, O. S., and A. J. Barduhn, "Hydrates of Iso- and Normal Butane and Their Mixtures," *Desalination*, **6**, 57 (1969).

Tee, L. S., S. Gotoh, and W. E. Stewart, "Molecular Parameters for Normal Fluids: The Kihara Potential with Spherical Core," *Ind. Eng. Chem. Fund.*, **5** (3), 363 (1966).

van der Waals, J. H., and J. C. Platteeuw, "Clathrate Solutions," *Adv. Chem. Phys.*, **2**, 1 (1959).

Vema, V. K., "Gas Hydrates from Liquid Hydrocarbon Wate Systems," Ph.D. Thesis, Univ. Michigan, Ann Arbor (1974).

Wu, B-J., D. B. Robinson, and H.-J. Ng, "Three- and Four-Phase Hydrate Forming Conditions in Methane + Isobutane + Water," *J. Chem. Thermo.*, **8**, 461 (1976).

Manuscript received February 23, 1983; revision received January 5, 1984, and accepted January 12.

Effect of Temperature on Crystallization and Dissolution Processes in a Fluidized Bed

The influence of temperature on crystallization and dissolution kinetics in a fluidized bed was investigated. Values of activation energies were determined and a correlation between the rate constants of secondary nucleation and of the surface integration step of crystal growth was presented.

JERZY BUDZ, P. H. KARPIŃSKI and ZBIGNIEW NURUĆ

Institute of Chemical Engineering and Heat Systems
Technical University of Wroclaw
Wroclaw, Poland

SCOPE

The Arrhenius equation is widely used to present the effect of temperature on kinetics of overall crystal growth, of dissolution, and of primary and secondary nucleation, despite the well-known fact that this equation is essentially valid for chemical reaction kinetics. Similarly, the driving force for crystallization—i.e., supersaturation—is usually expressed in terms of absolute concentration difference but not, as theoret-

Piotr H. Karpiński is presently at the Department of Chemical Engineering, Worcester Polytechnic Institute, Worcester, MA 01609.

ically recommended, in terms of relative supersaturation even when data concerning different hydrodynamic and/or temperature conditions are compared.

The aim of this work is to show that the above uncritical approaches may give a false picture when temperature effect is studied and to propose a more appropriate solution.

Kinetics of growth, dissolution, and secondary nucleation of two inorganic salts, aluminum potassium sulfate and sodium thiosulfate, were investigated in a laboratory-scale fluidized bed apparatus over the temperature ranges 286–327 K and 286–309 K. The measuring technique was the same as in previously reported hydrodynamic studies (Karpiński, 1981).

CONCLUSIONS AND SIGNIFICANCE

The rate constants of kinetic equations for the dissolution of crystals, for the diffusion step of crystal growth, and for the surface reaction step of crystal growth were found to be related with temperature according to the Arrhenius equation. This equation, however, was shown not to be applicable for the secondary nucleation rate constant.

The growth of sodium thiosulfate crystals was found to be diffusion-controlled, whereas for aluminum potassium sulfate the contribution of the diffusion step increases with the increase of temperature.

Secondary nucleation and crystal growth were assumed to be competitive processes and, based on this assumption, a simple model was proposed. This model clarifies the indirect effect of temperature on secondary nucleation kinetics that concerns solely the interrelated surface reaction step of crystal growth. It was shown that the use of absolute supersaturation as the driving force for crystallization may lead to entirely false conclusions, and therefore the use of relative supersaturation is strongly recommended.

INTRODUCTION

Crystal Growth and Dissolution

Kinetics of both the crystal growth and the dissolution processes may be described by the well-known relationships between mass rates and supersaturation:

$$\dot{m} = k_G A(\Delta c)^g \tag{1}$$

and

$$\dot{m} = k_D A(-\Delta c) \tag{2}$$

respectively. It has been reported (Nývlt et al., 1964; Bliznakov et al., 1971; Garside and Mullin, 1968; Mullin and Gaska, 1969; Helt and Larson, 1977; Randolph and Cise, 1972) that the influence of temperature on the rate constants k_G and k_D, over a moderately wide range of temperature, may be expressed in a form of the Arrhenius equation:

$$\frac{d\ \ln k}{dT} = \frac{E}{RT^2} \tag{3}$$

As far as the effect of temperature on dissolution kinetics is considered, such an approach seems to be theoretically correct, assumed that it is a simple mass transfer process from the crystal surface to the bulk solution. In the case of crystal growth, however, such a way cannot be theoretically supported since this process is much more complex, and when a simple two-step crystal growth concept is adopted, it consists of two consecutive steps:

(i) diffusion of growth units to the boundary of the Volmer layer (adsorption layer) with the mass rate:

$$\dot{m} = k_d A(w - w_i) \tag{4}$$

(ii) incorporation of ions (particles) into the crystal lattice, frequently referred to as the surface reaction step, with the mass rate:

$$\dot{m} = k_r A(w_i - w_{eq})^r \tag{5}$$

The overall mass rate of crystal growth:

$$\dot{m} = k_G A(w - w_{eq})^g$$

depends on contributions from each step, each of which may also vary with temperature. If both rate constants k_d and k_r are assumed to satisfy the Arrhenius equation, then the so-called overall activation energy for crystal growth E_G is the resultant of activation energies of both steps; this is probably why the dependence of E_G on temperature has been reported (in order words, the Arrhenius plot has been found to be curvilinear). Despite its weak theoretical background, the value of E_G is very often compared with that of E_d, the latter found from independent dissolution measurements, to determine which of the growth process steps is the controlling step. Van Hook (1959) compared values of E_G, E_d, and E_η (the activation energy for viscosity), for a sucrose-water system. He showed that at low temperatures $E_G \gg E_d$ and $E_G \gg E_\eta$, thus the growth takes place within the kinetic regime. In contrast, for temperatures greater than 333 K values of all three energies were comparable with the increased contribution of the diffusion step. Analogous results were reported by Rumford and Bain (1960) for NaCl-water system. In this case, 353 K was found to be a transition temperature. Similar comparison by Mullin and Gaska for K_2SO_4($E_G = 1.8 \times 10^4$ J/mol, $E_d = 2 \times 10^4$ J/mol) led these authors to the conclusion that within the temperature range 293–353 K diffusion-controlled growth takes place. Garside and Mullin (1968) assumed $r = 2$ and applied the results of dissolution tests for K-alum (i.e., assumed $k_D = k_d$) and have shown that the surface reaction rate constant k_r satisfies the Arrhenius equation. They found $E_R = 4.3 \times 10^4$ J/mol and $E_D = 1.2 \times 10^4$ J/mol. The interpretation of experimental data reported so far is correct provided that the surface reaction order r is constant and independent of temperature. There are many reports, however, which show local minima and maxima when the growth rates were plotted against the temperature. Such a phenomenon has, among others, been observed for KCl, KNO_3, $NaNO_2$, $NaNO_3$, $NaClO_4$, and K-alum and has been explained by the thermic change of the supersaturated solution structure at the crystal surface due to changes in the dehydration rate. When a small amount of ethanol was added to an aqueous salt solution, the temperature effect was compensated for, since ethanol itself influences the water structure.

Secondary Nucleation

In the case of primary, heterogeneous nucleation, Nývlt (1971) recommended the following equation:

$$\frac{d\ \ln k_{N,het}}{dT} = \frac{E_{N,het}}{RT^2} \tag{6}$$

where $k_{N,het}$ is the rate constant of the kinetic equation:

$$\dot{N}_{het} = k_{N,het}(\Delta c)^n \tag{7}$$

The experimental results, however, did not validate the equation.

The numerical rate of secondary nucleation is usually expressed as:

$$\dot{N} = k_N(\Delta c)^n \mu_i^j \tag{8}$$

Desai et al. (1974) showed that any of the distribution moments may be used in Eq. 8 since they are interrelated mathematically. The secondary nuclei can be produced due to the collision mechanism (Clonz and McCabe, 1972; Johnson et al., 1972) and/or they may be bred from the adsorption layer (Sung et al., 1973). In both cases the crystal surface itself or the adsorption layer immediately adjacent to the crystal surface is the source of nuclei. Thus, the second moment of distribution, i.e., the area of the parent crystals, may be chosen (Karpiński, 1981) to represent the distribution moment in Eq. 8:

$$\dot{N} = k_N A(\Delta w)^n \tag{8a}$$

In the course of the past decade many papers on secondary nucleation have been published but only small numbers of them were concerned with the temperature effect. Helt and Larson (1977) investigated the secondary nucleation of KNO_3. They found that the activation energies are: $E_G = 3.1 \times 10^4$ J/mol and $E_N = -10.8 \times 10^4$ J/mol. Their results were consistent with those of Genck and Larson (1972) for the same system and of Sikdar and Randolph (1976) for K_2SO_4 and $MgSO_4 \cdot 7H_2O$. The explanation of the fact that the nucleation rate decreases as temperature increases given by Helt and Larson indicates that at elevated temperatures a smaller number of growth units are present within the adsorption layer due to their temperature-facilitated incorportion into the crystal lattice. A similar mechanism has been proposed by Mullin and Leci (1969) for citric acid.

The existing opinions may be briefly outlined as follows. Both the growth and the secondary nucleation processes are competitive; since the growth rate is more rapid at elevated temperatures, the resulting nucleation rate appears slower. Based on the mixed suspension, mixed product removal (MSMPR) crystallizer concept, Wey and Terwilliger (1980) reviewed literature reports concerning the influence of temperature on the secondary nucleation. According to their conclusions the relation between two ratios—that of the activation energies E_N/E_G and that of the relative nucleation order $i = n/g$—may be used to predict the existence of the relative variation between the nucleation and growth rates as well as the direction of change in these rates with temperature. Their model explains well the experimental results but it is not essential in understanding mechanisms of such changes. These authors also have not taken into consideration the fact that the change in hydrodynamic conditions due to variations of the viscosity and density with temperature may cause even wider changes in the nucleation rate than those caused by temperature.

Driving Force

The thermodynamic driving force for crystallization is a difference of the chemical potential

$$\Delta\mu = \mu - \mu_{eq} \tag{9}$$

which expressed in terms of supersaturation ratio is (Mullin 1979):

$$\Delta\mu = RT \ln \frac{a^{\pm}}{a^{\pm}_{eq}} = \nu RT \ln \left(\frac{c}{c_{eq}} \frac{\gamma}{\gamma_{eq}} \right) = \nu RT \ln \left(S \frac{\gamma}{\gamma_{eq}} \right) \tag{10}$$

Assuming that: (i) $\Delta\mu$ is independent of degree of dissociation, (ii) the ratio of the activity coefficients is unity, and (iii) over the whole supersaturation range the following relation holds:

$$\ln S = \ln(1 + \sigma) \approx \sigma \tag{11}$$

Eq. 9 may be simplified to:

$$\frac{\Delta\mu}{\nu RT} = \sigma \tag{12}$$

Since values of the activity coefficient are rarely available, molar or mass units of concentration with preference to those which concern hydrates rather than anhydrous bases are recommended (Mullin). The use of properly defined supersaturation is of great importance. The absolute difference of concentrations as a measure of supersaturation must not be used since it strongly depends on the temperature, e.g.,

$$\Delta w = \sigma w_{eq}(T) \tag{13}$$

and can even lead to false conclusions, as will be shown later. Unfortunately many authors neglect this importance.

Kinetic Equations

Taking into account the recommendations of the preceding section concerning the driving force, the following kinetic equations were used:
For the mass growth flux:

$$\dot{m}_G = k_G \sigma^g = \frac{3}{\beta t_G} \left\{ \left[\frac{(\alpha\rho_c)^2 m_e}{N} \right]^{1/3} - \left[\frac{(\alpha\rho_c)^2 m_i}{N} \right]^{1/3} \right\} \tag{14}$$

For the mass dissolution flux:

$$\dot{m}_D = k_D(-\sigma) \tag{15}$$

For determination of k_r and k_d from Eqs. 4 and 5 (Karpiński 1980), for $r = 2$:

$$\frac{\sigma}{\sqrt{\dot{m}_G}} = \frac{1}{k_d} \sqrt{\dot{m}_G} + (k_r)^{-0.5} \tag{16}$$

For the numerical flux of the secondary nucleation (Karpiński 1982):

$$\dot{N}_A = k_N \sigma^n = \frac{\bar{N}_{sec} \dot{V}}{N V_c \beta L_e^2} \tag{17}$$

EXPERIMENTAL

Equipment and Procedure

As diagrammed in Figure 1, the research apparatus was a laboratory-scale fluidized bed crystallizer (1) of 0.048 m ID, a sampling cell (2) for the secondary nucleation measurements, and associated controlled heating and cooling systems. A fluidized bed of uniformly sized crystals provides the well-defined hydrodynamics requirement. The working temperature level in the crystallizer was kept with an accuracy 0.02 K. Detailed description of the equipment was presented elsewhere by Naruć (1982).

The experimental procedure adopted (Karpinski, 1982) can be described briefly as follows. Both working temperature and flow rate in the apparatus were maintained constant by the control system. A known mass and number of crystals, usually 6.0–7.0 g, of a known uniform size was placed in the crystallizer. The crystals formed a fluidized bed and grew for a definite period of time. The solution carrying the secondary nuclei generated in the bed flowed through the sampling cell. At the required moment the cell was cut off instantaneously by a three-way stopcock, disconnected from the system, and placed in a water bath at the working temperature of the crystallizer; the nuclei seized in the cell were allowed to grow, up to a size visible under the microscope. At the same time the grown crystals were removed, filtered, rinsed with acetone, and dried. The number of nuclei in the cell was counted. The secondary nucleation and growth fluxes were determined from Eqs. 17 and 14, respectively. The dissolution fluxes were determined in a similar manner (the cell, however, was not used during the dissolution experiments). To assure maximum accuracy of the results, the surroundings of both the crystallizer and the sampling cell were thermostatically controlled to maintain the ambient temperature at a level 3–5 K below the working temperature in the crystallizer. The dissolution, growth, and secondary nucleation rates were measured for two salts, $KAl(SO_4)_2 \cdot 12H_2O$ and $Na_2S_2O_3 \cdot 5H_2O$, over the temperature range from 286 K to 327 K and from 286 K to 309 K. The superficial velocities of solution in the growing section of the crystallizer were 0.029 m/s for K-alum and 0.015 m/s for thiosulfate.

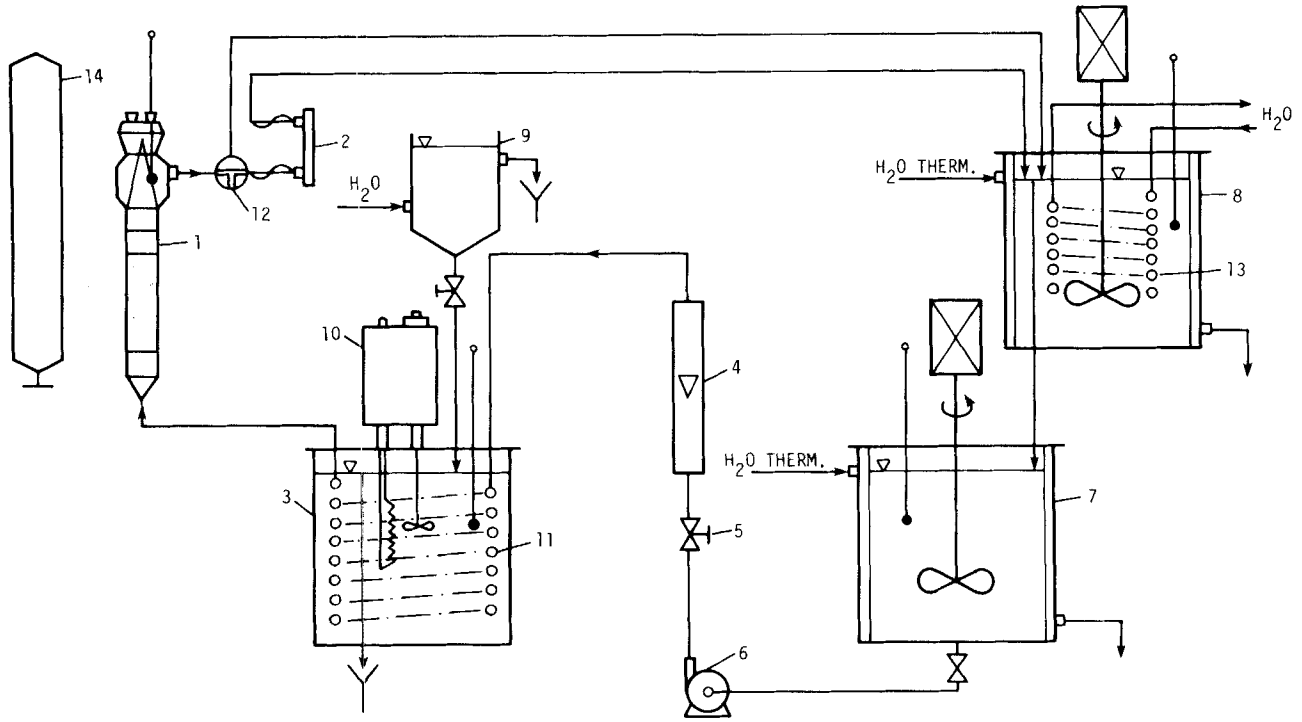

Figure 1. Experimental apparatus: 1. Crystallizer; 2. Cell; 3. Cooling tank; 4. Rotameter; 5. Control valve; 6. Feed pump; 7. Feed tank; 8. Dissolving tank; 9. Cooling water head tank; 10. Thermostat; 11. Cooling coil; 12. Three-way stopcock; 13. Heating coil; 14. Radiant heater.

RESULTS AND DISCUSSION

Crystal Growth and Dissolution

Results of crystal growth measurements for K-alum are presented in Figure 2 and collective results of crystal growth and dissolution for $Na_2S_2O_3 \cdot 5H_2O$ are shown in Figure 3. An example of the application of Eq. 16 for K-alum crystal growth is graphically represented in Figure 4. Values of constants in Eqs. (14)–(17) are collected in Table 1.

Even a preliminary analysis of the K-alum growth data at temperataures $T_5 = 318$ K and $T_6 = 327$ K suggests that a change in the growth mechanism between these temperatures may take place. The slope of the respective straight lines in Figure 2 and values of both the overall growth rate constant k_G and the mass transfer coefficient k_d differ considerably from their values corresponding to the lower temperatures. There is a general rule (Karpiński 1981) that if the surface reaction order r is properly chosen, the correlation errors of Eq. 16 are smaller than those of Eq. 14. As may be seen from Table 1, this rule is also validated for all temperatures below 318 K. Thus it seemed that the surface reaction order for temperatures exceeding 318 K is no longer equal to 2. To determine an appropriate value of the surface reaction

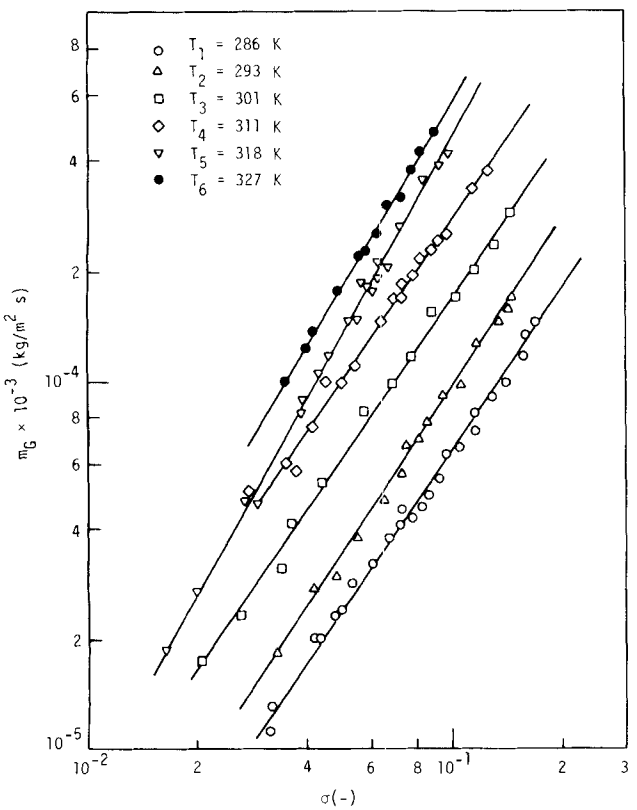

Figure 2. Mass growth flux versus relative supersaturation for K-alum.

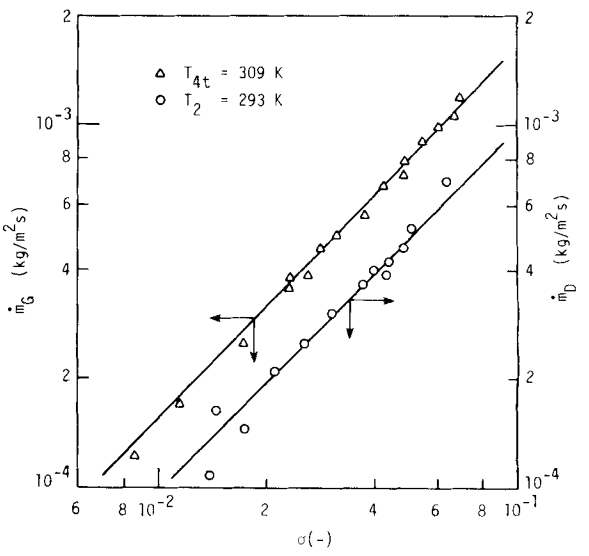

Figure 3. Mass growth flux (Δ) versus relative supersaturation, and dissolution flux (o) versus relative supersaturation for $Na_2S_2O_3 \cdot 5H_2O$.

TABLE 1. CONSTANTS OF THE KINETIC EQS. 14–17 AND ASSOCIATED CORRELATION ERRORS

		Salt									
		$KAl(SO_4)_2 \cdot 12H_2O$						$Na_2S_2O_3 \cdot 5H_2O$			
		Series									
		I	II	III	IV	V	VI	It	IIt	IIIt	IVt
		Temperature, K									
Quantity	Units	286	293	301	311	318	327	286	293	301	309
$k_G \times 10^3$	kg/m²·s	1.77	2.97	4.64	7.07	25.4	25.9	8.07	10.1	10.6	11.1
g	—	1.44	1.49	1.44	1.42	1.76	1.66	1.0	1.0	1.0	1.0
s_G	%	6.5	5.3	5.9	7.4	6.3	2.6	5.4	11.6	7.3	4.8
R_G	—	0.997	0.998	0.998	0.992	0.997	0.999	0.997	0.983	0.996	0.999
$k_D \times 10^3$	kg/m²·s	1.77	—	4.00	5.58	8.12	—	8.22	9.78	11.0	10.8
s_D	%	11.4	—	5.2	3.3	4.9	—	11.3	10.7	4.8	9.8
R_D	—	0.991	—	0.996	0.999	0.998	—	0.996	0.982	0.998	0.996
$k_d \times 10^3$	kg/m²·s	1.48	2.31	3.48	5.74	18.9*	19.7*				
$k_r \times 10^2$	kg/m²·s	2.11	2.84	6.33	9.75	7.2*	10.6*	See constants			
s_{d-r}	%	4.2	3.3	3.6	5.0	9.3*	3.7*	k_G, g, s_G, R_G			
R_{d-r}	—	0.996	0.972	0.981	0.926	0.854*	0.928*	for growth			
$k_N \times 10^{-6}$	$m^{-2} \cdot s^{-1}$	4.49	4.02	7.37	9.29	13.3	10.2	0.139	0.151	0.180	0.080
n	—	2.03	1.91	2.10	2.12	2.18	2.17	1.88	1.69	1.88	1.70
s_N	%	12.5	14.1	15.1	24.4	16.5	17.3	13.2	25.5	25.6	51.7
R_N	—	0.998	0.988	0.994	0.985	0.981	0.988	0.991	0.893	0.980	0.911

*) Values for $r = 2$; see Table 2 for real values.

order the following procedure was adopted. The Arrhenius plot (Figure 5) was constructed and the extrapolated values for k_d, symbolized as k'_d, were used to calculate the relative driving force for the diffusional step of the growth, based on

$$\sigma'_d = \frac{\dot{m}_G}{k'_d} \tag{18}$$

for all the measuring points of series V and VI. Finally, by means of the least squares method, the real values of the constants k'_r and r' of the equation

$$\dot{m}_G = k'_r(\sigma - \sigma'_d)^{r'} = k'_r(\sigma'_i)^{r'} \tag{19}$$

were found. The results are shown in Table 2. The comparison of the mean square relative errors s'_{d-r} and the coefficients of correlation R'_{d-r} from Table 2 with those for s_G and R_G from Table 1 is self-explanatory. It is noticeable that the resulting surface reaction order r' is the same for both series V and VI. The anomalies in the crystal growth of K-alum above 318 K have also been observed by Chernov et al. (1977), who investigated growth of different faces of a single crystal at very high turbulence of the solution flowing past crystal surface. Thus it may be accepted that only the mechanism of the surface reaction has been changed when the temperature has exceeded the transition value. These authors suggested that the observed effect resulted from the change of the solution structure as well as the presence of admixtures and dissolved gases. Wojciechowski (1982) has shown that the hydration degree of ions in aqueous solutions is very sensitive to changes of temperature between 315 and 320 K. Therefore it may be assumed that the

TABLE 2. MASS TRANSFER COEFFICIENT AND SURFACE REACTION CONSTANT RATE FOR GROWTH OF K-ALUM ABOVE 318 K

Constant: Temperature	$k'_d \times 10^3$ kg/m²·s	k'_r kg/m²·s	r'	s'_{d-r} %	R'_{d-r}
318 K	7.57	1.14	2.63	4.1	0.956
327 K	10.8	1.32	2.63	2.0	0.989

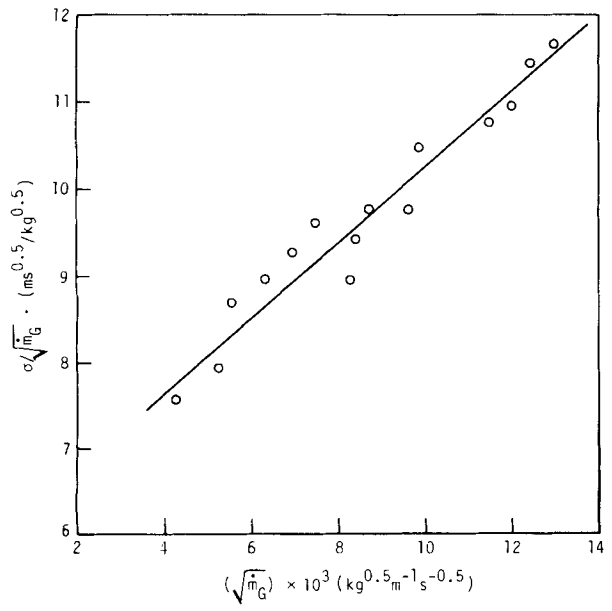

Figure 4. Graph illustrating the use of Eq. 16. Data for growth of K-alum, Series II, $T = 293$ K.

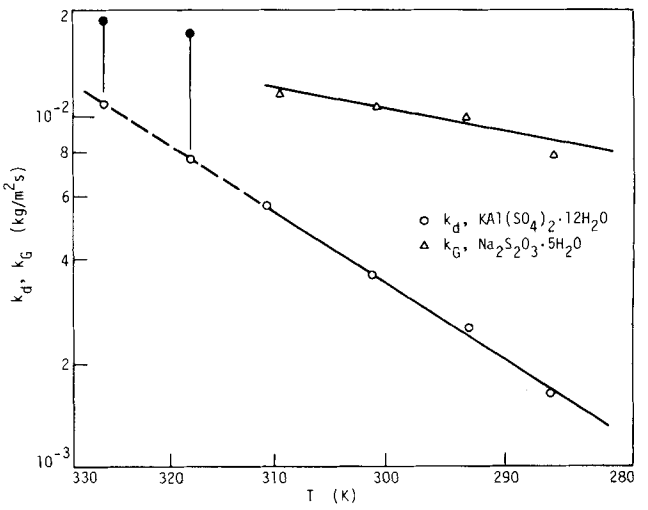

Figure 5. Plot of Arrhenius Eq. 3 for the diffusion step of crystal growth.

TABLE 3. VALUES OF ACTIVATION ENERGIES AND ASSOCIATED CORRELATION ERRORS FOR GROWTH AND DISSOLUTION OF K-ALUM AND $Na_2S_2O_3 \cdot 5H_2O$

	Activation energy/(S_E) J/mol			
	$E_G \times 10^{-4}$	$E_d \times 10^{-4}$	$E_R \times 10^{-4}$	$E_D \times 10^{-4}$
K-alum (286–311)K	—	3.6 (1.4%)	5.0 (9.7%)	3.2 (3.7%)
$Na_2S_2O_3 \cdot 5H_2O$ (286–309)K	1.2 (10.5%)	1.1 (1.6%)	—	1.1 (1.6%)

changes in the surface reaction order of K-alum observed above 318 K are caused by recombination of ion-water complexes, which presumably takes place around this temperature. For these reasons series V and VI will essentially be omitted in further data analysis since they are governed by other surface reaction mechanism.

$Na_2S_2O_3 \cdot 5H_2O$ was investigated below its first phase transition, i.e., below 322 K. This case differs from that of K-alum in that the overall order of Eq. 14 is equal to unity and the straight lines of the Eq. 16 intersect the ordinate very close to the 0 point. This physically means that the surface reaction is very rapid and that all the mass transfer resistance is due to the diffusional step of the crystal growth. Furthermore, it also means that k_G is equal to k_d. The Arrhenius equation for the growth of the thiosulfate is graphically presented in Figure 5.

The values of the activation energies and the associated correlation errors for growth and dissolution of both salts are presented in Table 3. When mass transfer coefficients for both growth and dissolution are compared in Figure 6, the resulting activation energy for both oppositely directed processes is 3.4×10^4 J/mol with an error of 7.7%. This result corroborates the fact, already stated from hydrodynamic consideration (Karpiński, 1981; Budz, 1982), that the basic equation of the method which allows us to determine the rate constants of the individual steps of the crystal growth (Karpiński, 1980):

$$\sigma(\dot{m}_G)^{-1/r} = \frac{1}{k_d}(\dot{m}_G)^{1-(1/r)} + (k_r)^{-1/r} \qquad (20)$$

is valid for the investigated salts.

Equation 20 is physically justified for $1.1 < r \leq 2.0$ (Karpiński, 1984).

When the surface reaction is very rapid, as it has been for the thiosulfate, one cannot expect Eq. 16 to be a source of exact values of k_r, since its reciprocal, which appears in Eq. 16, is very close to zero. On the other hand, it is thus very sensitive to any variation of the slope of the correlation straight line, due to the simple dispersion of the experimental points. This is why only k_r for K-alum will be considered. The k_r constant depends on temperature, as predicted by the Arrhenius equation (Figure 7). The activation energy found for series V and VI, calculated for $r = 2.63$, is $E'_R = 1.5 \times 10^4$ J/mol.

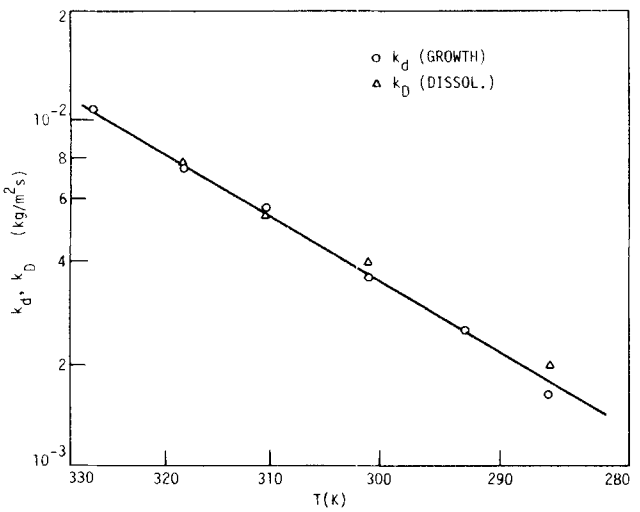

Figure 6. Comparison of diffusion step rate constant and dissolution mass transfer coefficient for K-alum.

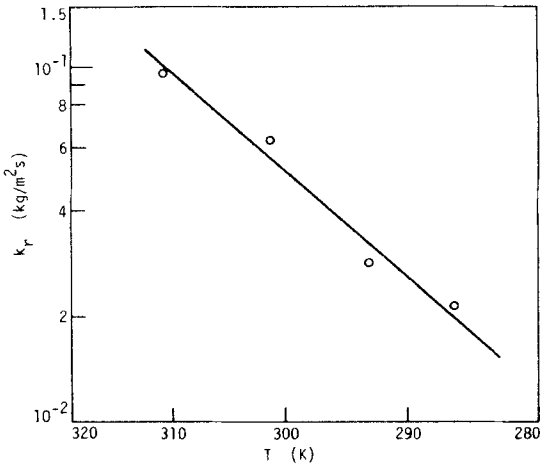

Figure 7. Plot of Arrhenius Eq. 3 for surface reaction rate constant for K-alum.

The importance using properly defined driving forces, as has been emphasized, may be seen from Figures 8 and 9 where the surface reaction constants $k_{r,\Delta c}$ and $k_{r,\Delta\omega}$ were calculated based on the absolute supersaturation units in kg of hydrate/m³ and in kg of hydrate/hg of H_2O, respectively. Both plots give a false picture. From Figure 8 it could be concluded that the kinetics of the surface reaction do not depend on the temperature, whereas Figure 9 suggests that the rate of the surface reaction is slower at elevated temperatures.

Secondary Nucleation

There is no doubt that secondary nucleation kinetics depend markedly on hydrodynamic conditions which actually characterize the crystallizer. Investigation of the effect of hydrodynamics on secondary nucleation of the K-alum, using the same apparatus (Budz, 1982), showed that the following equation holds:

$$\dot{N}_A = 1.9 \times 10^{-5} Re^{2.11} \dot{m}_G \qquad (21)$$

Analogous results were also obtained for $Na_2S_2O_3 \cdot 5H_2O$ (Budz) and for $CuSO \cdot 5H_2O$ and $MgSO_4 \cdot 7H_2O$ (Karpiński, 1981). Budz suggested that the Reynolds number defined as

$$Re = \frac{uL_{eA}\rho_l}{\eta\epsilon_e} \qquad (22)$$

where the mean crystal size was defined as

$$L_{eA} = L_e \frac{\sqrt{\beta}}{\pi} \qquad (23)$$

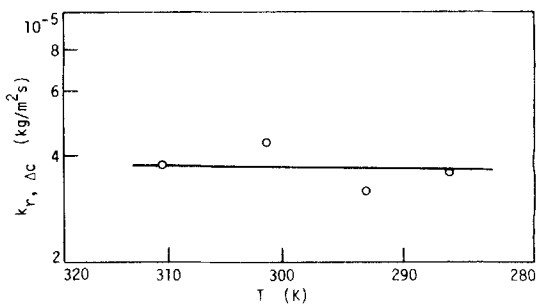

Figure 8. Surface reaction rate constant based on driving force expressed by absolute supersaturation in mol/m³ vs. reciprocal absolute temperature for K-alum.

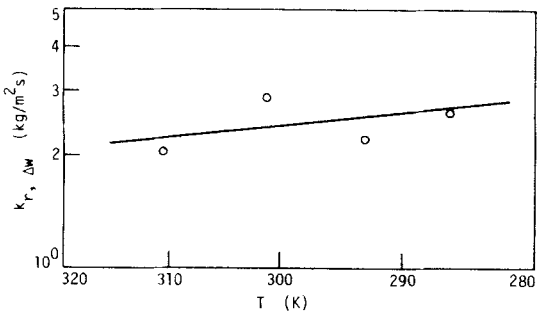

Figure 9. Surface reaction rate constant, based on driving force expressed by absolute supersaturation in kg of hydrate/kg of water vs. reciprocal absolute temperature for K-alum.

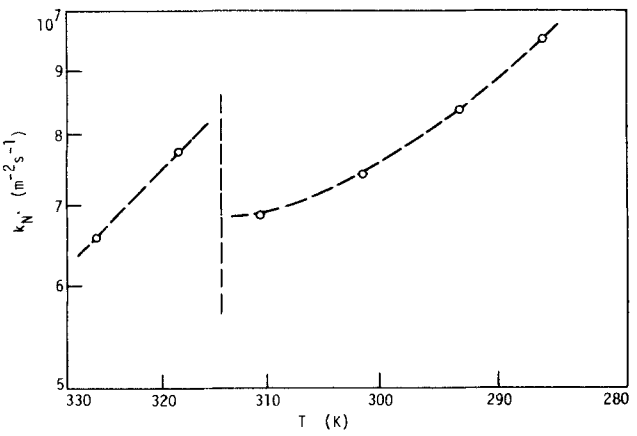

Figure 10. Secondary nucleation rate constant vs. reciprocal absolute temperature for K-alum.

best describes the hydrodynamic conditions in the case of secondary nucleation occurring in a fluidized bed. Therefore, when the thermal effect is studied, all measurements are to be carried out at the same Reynolds number. It is, however, very difficult in practice to maintain the Reynolds number constant while simultaneously changing the temperature, since the former depends on properties very sensitive to temperature variations. The secondary nucleation data were thus reduced to a constant Reynolds number (the average Reynolds number for all experiments). The simple reduction procedure based on Eq. 21 is described elsewhere (Naruć, 1982).

Since the secondary nucleation order remained practically constant for K-alum (Table 1) it was possible to compare the secondary nucleation rate constant based on the average nucleation order $n = 2.09$. The corresponding plot of k_N versus the reciprocal absolute temperature is shown in Figure 10. It is obvious that the Arrhenius equation does not apply in this case.

Particularly interesting is the fact that the discontinuity of the plot is observed above 318 K, that is above the same temperature

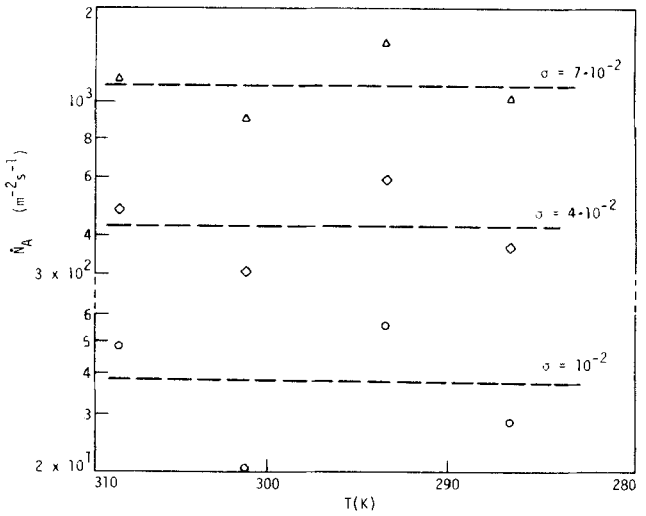

Figure 11. Secondary nucleation flux at constant supersaturation levels vs. reciprocal absolute temperature for $Na_2S_2O_3\cdot5H_2O$.

as observed for the surface reaction rate constant. This seems to suggest that both rate constants are interrelated and, accordingly, the secondary nucleation process and the surface reaction of the crystal growth are also physically interrelated. For sodium thiosulfate, as may be seen from Figure 11, the secondary nucleation flux does not depend on temperature with restriction to the accuracy of the experimental procedure. This conclusion will be further supported later.

Values of activation energies for K-alum obtained in this study are compared in Table 4 with those reported by various authors (there are no such data available for sodium thiosulfate). As it follows from Table 4, data obtained may be compared with those by Garside and Mullin only. The values of E_R are conformable, whereas the values of E_D are not consistent since they were obtained under different hydrodynamic conditions.

Secondary Nucleation and Crystal Growth as Competitive Processes

Figure 12 shows the relation between the secondary nucleation rate constant and the surface reaction rate constant for K-alum. The linearized form of the correlation is as follows:

$$k_N = a + \frac{b}{k_r} \tag{24}$$

Since, as has already been stated,

$$k_r = k_{ro} \exp\left(-\frac{E_R}{RT}\right) \tag{25}$$

the graph $\ln(k_N - a)$ vs. $(1/T)$ should result in a straight line. The plot is presented in Figure 13 and the corresponding equation is

TABLE 4. COMPARISON OF VALUES OF ACTIVATION ENERGIES FOR CRYSTALLIZATION AND DISSOLUTION OF K-ALUM OBTAINED BY VARIOUS AUTHORS

Authors	Range of temperatures K	E_G	E_d	E_R $\times10^4$ J/mol	E_D	E_N
Garside and Mullin (1968)	$288 < T < 320$	—	—	4.3	1.2	—
Rousseau and McCabe (1976)		2.5	—	—	—	5.0
Rousseau and Woo (1980)	$304 < T < 306$	3.2	—	—	—	10.1
	$286 < T < 318$				3.2	
This paper	$286 < T < 311$	*	3.6	5.0		**
	$311 < T < 327$			1.5		

* Overall growth activation energy has no physical meaning since $g \neq 1.0$.
** The Arrhenius equation was found to be not applicable.

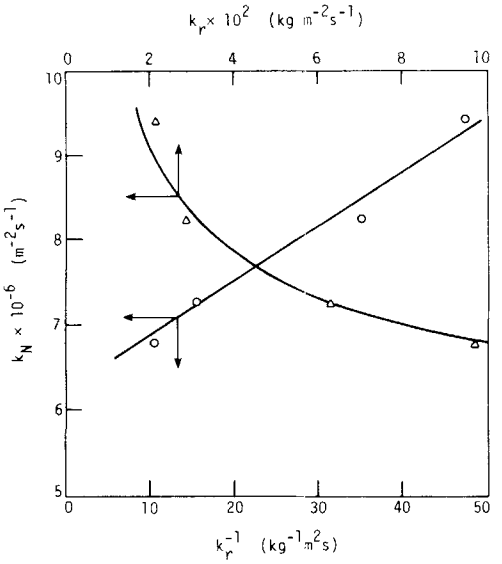

Figure 12. Direct and linearized dependence of secondary nucleation rate constant on surface reaction rate constant.

$$\ln(k_N - 6.1 \times 10^6) = 6.0 + \frac{6{,}010}{T} \qquad (26)$$

with an error $s_y = 3.2\%$ and the coefficient of correlation $R = 0.999$. When the values of the activation energies for K-alum found for $T > 318$ K and for $T < 318$ K—which are $E_R = 1.5 \times 10^4$ J/mol and $E_R = 5 \times 10^4$ J/mol, respectively—are compared, the decrease of the secondary nucleation rate for increasing temperature should be more pronounced for temperatures above 318 K. The results shown in Figure 13 verify this deduction.

For thiosulfate it has been stated that the surface reaction is very rapid and that k_r takes on a high numerical value. Evaluating the righthand side of Eq. 24 in the limit as k_r approaches infinity, we obtain k_N equal to a constant a that also corroborates the legitimacy of the assumed model, Eq. 24. The constant a and the term b/k_r may have a certain physical meaning when it is assumed that:

1. There are two sources of the secondary nuclei, the crystal surface and the adsorption layer immediately adjacent to the surface.
2. There are two mechanisms according to which nuclei can be transferred to the solution in a fluidized bed: the collision mechanism and the fluid shear mechanism (Karpiński, 1981; Budz, 1982).
3. The quality of the parent crystal surfaces remains unaltered during investigation (i.e., the concentration of micro-roughnesses on crystal surfaces is statistically constant).
4. In the case when nuclei are produced from the adsorption layer, "competition" between the secondary nucleation and the crystal growth takes place: an increase of k_r results in a slower secondary nucleation rate and conversely, a decrease of k_r results in faster secondary nuclei production.

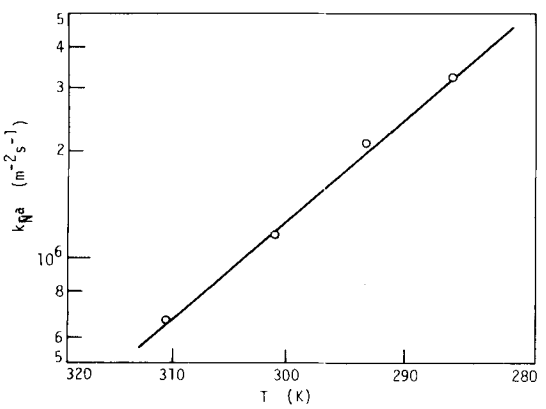

Figure 13. Verification of model Eq. 24 for K-alum. Ln ($k_N - a$) ploted vs. 1/T.

Under such assumptions the constant a of Eq. 24 represents the part of the total secondary nucleation flux that originates directly from the crystal surface and thus is independent of temperature. On the other hand the term b/k_r represents that part of the total secondary nucleation flux which originates from the adsorption layer and, since k_r depends on temperature according to the Arrhenius equation (Eq. 25), it undergoes changes in accordance with the temperature. It is similarly obvious that in the case of a very rapid surface reaction this term becomes zero and no temperature effect on the nucleation rate is to be expected. In the case of a moderate rate of surface reaction, a decrease in the nuclei formation rate, according to Eq. 26, will take place. The results obtained for both investigated salts verify the proposed model.

CONCLUSIONS

Equation 20, based on the two-step crystal growth concept, explains experimental results concerning crystal growth with better accuracy than the classic power law, Eq. 1. It also gives values of both the mass transfer coefficient and the surface reaction rate constants which are very useful in the further elaboration of experimental data. The values of the mass transfer coefficient for the diffusion step of crystal growth obtained by means of this equation are consistent with corresponding value of the mass transfer coefficient for dissolution, regardless of temperature.

All the three rate constants k_d, k_r and k_D are related to temperature according to the Arrhenius equation. The comparison of the activation energies for K-alum indicates that with the increase of temperature the contribution of the surface reaction decreases and the diffusion step plays a more important role. The growth of sodium thiosulfate is diffusion-controlled since the surface reaction is very rapid in this case.

For temperatures above 318 K the surface reaction mechanism of K-alum crystal growth undergoes a change. The surface reaction order is no longer equal to 2; its value amounts to 2.63, a change that seems to be caused by the change of the solution structure.

The effect of temperature on secondary nucleation kinetics is not direct and it concerns solely the interrelated surface reaction step. A model, Eq. 24, verified experimentally for both investigated salts, explains why the Arrhenius equation cannot be applied for the secondary nucleation rate constant.

The application of an appropriate driving force in kinetic equations when the temperature effect is studied, deserves special attention. The relative supersaturation in terms of molar (or mass) concentrations of hydrate should preferably be used. The use of absolute concentration differences as the driving force may lead to false conclusions.

In general the effect of hydrodynamic conditions on the secondary nucleation rate is much more evident than that of temperature. The effect of temperature is fully distinguishable if the appropriate reduction of secondary nucleation data to standard (or average) hydrodynamic conditions has been assured.

NOTATION

a = constant in Eq. 24
$a^{\pm}$ = mean ionic activity
$a^{\pm}_{eq}$ = mean ionic equilibrium activity
b = constant in Eq. 24
c = concentration, mol/m^3
c_{eq} = equilibrium concentration, mol/m^3
Δc = absolute supersaturation, mol/m^3
E = molar activation energy, J/mol
E_d = molar ativation energy for diffusion step of crystal growth, J/mol

E_D = molar activation energy for dissolution, J/mol
E_N = molar activation energy for nucleation, J/mol
$E_{N,het}$ = molar activation energy for primary heterogeneous nucleation, J/mol
E_G = molar activation energy for overall crystal growth, J/mol
E_R = molar activation energy for surface reaction step of crystal growth, J/mol
g = overall growth order
i = relative nucleation order, $i = n/g$
j = exponent in Eq. 8
k = rate constant
k_d = mass transfer coefficient, kg/m^2·s
k_D = dissolution rate constant, kg/m^2·s
k_G = overall growth rate constant, kg/m^2·s
k_N = secondary nucleation rate constant, m^{-2}·s^{-1}
$k_{N,het}$ = primary heterogeneous nucleation rate constant, m^{-2}·s^{-1}
k_r = surface reaction rate constant, kg/m^2·s
k_{r0} = frequency factor, kg/m^2·s
L_e = final crystal size, m
L_{eA} = equivalent crystal size, Eq. 23, m
m_e = final mass of crystals, kg
m_i = initial mass of crystals, kg
$\dot{m}$ = mass growth rate, kg/s
$\dot{m}_D$ = mass flux for dissolution, kg/m^2·s
$\dot{m}_G$ = mass flux for crystal growth, kg/m^2·s
n = nucleation order
N = number of crystals
$\bar{N}_{sec}$ = mean number of nuclei in a cell
$\dot{N}$ = numerical rate of secondary nucleation, s^{-1}
$\dot{N}_{het}$ = numerical rate of primary heterogeneous nucleation, s^{-1}
$\dot{N}_A$ = numerical flux of secondary nuclei, m^{-2}s^{-1}
r = surface reaction order
R = universal gas constant, 8.315 J/mol K
R_{d-r} = coefficient of correlation, Eq. 16
R_D = coefficient of correlation, Eq. 15
Re = Reynolds number, Eq. 22
R_G = coefficient of correlation, Eq. 14
R_N = coefficient of correlation, Eq. 17
s_{d-r} = mean square relative error, Eq. 16,%
s_D = mean square relative error, Eq. 15,%
s_E = mean square relative error, Eq. 3,%
s_G = mean square relative error, Eq. 14,%
s_N = mean square relative error, Eq. 17,%
S = supersaturation ratio
t_G = duration of crystals growth time, s
T = absolute temperature, K
u = superficial velocity of solution, m/s
V_c = volume of cell, Figure 1, m^3
$\dot{V}$ = volumetric flow rate of solution, m^3/s
w = concentration, in kg of hydrate/kg H_2O
w_{eq} = equilibrium concentration (solubility), kg/kg
w_i = interfacial concentration, kg/kg
Δw = supersaturation, kg/kg

Greek Letters

α = volume shape factor
β = surface shape factor
γ = activity coefficient
γ_{eq} = equilibrium activity coefficient
Δ = increment
ϵ_e = final porosity of a fluidized bed
η = viscosity, Pa·s
μ = chemical potential, J/mol
μ_{eq} = equilibrium chemical potential, J/mol
μ_i = ith moment of distribution
$\Delta\mu$ = difference of chemical potential, J/mol
ν = number of moles of ions in 1 mole of solute
ρ_c = density of crystal, kg/m^3
ρ_l = density of solution, kg/m^3
σ = relative supersaturation
σ_d = relative supersaturation for diffusional step of crystal growth
σ_i = relative supersaturation for reaction step

LITERATURE CITED

Bliznakov, G., E. Kirkova, and R. Nikolayeva, "A Study of the Rate-Controlling Stage of the Process of Crystal Growth in Solutions," *Kristall u. Technik*, **6**, 33 (1971).

Budz, J., "Effect of Hydrodynamics on Crystallization and Dissolution Kinetics of Inorganic Salts in a Fluidized Bed," (in Polish) PhD Thesis, Tech. Univ. of Wroclaw, Poland (1982).

Chernov, A. A., et al., "Anomalous Temperature Dependence and Growth Rate Fluctuation of K-alum and KNO_3 Crystals," (in Russian) *Rost Krist.*, **12**, 103 (1977).

Clonz, N. A., and McCabe, W. L., "Contact Nucleation of Magnesium Sulfate," *Chem. Eng. Prog. Symp. Ser.*, **67**(110), 6 (1972).

Desai, R. M., J. W. Rachow, and D. C. Timm, "Collision Breeding: A Function of Crystal Moments and Degree of Mixing," *AIChE J.*, **20**, 43 (1974).

Garside, J., and J. W. Mullin, "The Crystallization of Aluminum Potassium Sulphate: A Study in the Assessment of Crystallizer Design Data. III: Growth and Dissolution Rates," *Trans. Inst. Chem. Eng.*, **46**, T11 (1968).

Genck, W. J., and M. A. Larson, "Temperature Effects on Growth and Nucleation Rates in Mixed Suspension Crystallization," *AIChE Symp. Ser.*, **68**(121), 57 (1972).

Helt, J. E., and M. A. Larson, "Effect of Temperature on the Crystallization of Potassium Nitrate by Direct Measurement of Supersaturaton," *AIChE J.*, **23**, 822, (1977).

Johnson, R. T., R. W. Rousseau, and W. L. McCabe, "Factors Affecting Contact Nucleation." *AIChE Symp. Ser.*, **68**(121), 31 (1972).

Karpiński, P. H., "Crystallization as a Mass Transfer Phenomenon," *Chem. Eng. Sci.*, **35**, 2,321 (1980).

———, *Mass Crystallization in a Fluidized Bed*, Ed. by Tech. Univ. of Wrocław, Poland (1981).

———, "Effect of Hydrodynamics on Secondary Nucleation and Growth Rates in a Fluidized Bed," *Industrial Crystallization '81*, S. J. Jančić and E. J. deJong, Eds., North-Holland Pub. Co., Amsterdam (1982).

———, "Verification of the Two-Step Growth Mechanism," *AIChE Ann. Meet.*, San Francisco (Nov., 1984).

Khamskii, E., *Crystallization in Chemical Industry*, (in Russian), Khimia, Moscow (1979).

Mullin, J. W., *Industrial Crystallization '78*, E. J. deJong and S. J. Jančić, Eds., North-Holland Publ. Co., Amsterdam (1979).

Mullin, J. W., and C. Gaska, "The Growth and Dissolution of Potassium Sulphate Crystals in a Fluidized Bed Crystallizer," *Can. J. Chem. Eng.*, **47**, 483 (1969).

Mullin, J. W., and C. L. Leci, "Evidence of Molecular Cluster Formation in Supersaturated Solutions of Citric Acid," *Phil. Mag.*, **19**, 1,075 (1969).

Naruć, Z., "Effect of Temperature on Crystallization and Dissolution Kinetics of Inorganic Salts in a Fluidized Bed," (in Polish) PhD Thesis, Tech. Univ. of Wrocław, Poland (1982).

Nývlt, J., J. Gotfried,and J. Křicková, "Crystallization. X: The Crystallization Rate of Urea," (in German) *Collection Czech. Chem. Commun.*, **29**, 161 (1964).

Nývlt, J., *Industrial Crystallization from Solution*, Butterworth, London (1971).

Randolph, A. D., and M. D. Cise, "Nucleation Kinetics of the Potassium Sulfate-Water System," *AIChE J.*, **18**, 798 (1972).

Rousseau, R. W., and W. L. McCabe, "Nucleation and Growth from Solution," World Cong. Chem. Eng., Amsterdam (1976).

Rousseau, R. W., and R. Woo, "Effects of Operating Variable on Potassium Alum Crystal Size Distribution," *AIChE Symp. Ser.*, **76**(193), 27 (1980).

Rumford, F., and J. Bain, "The Controlled Crystallization of Sodium Chloride," *Trans. Inst. Chem. Eng.*, **38**, 10 (1960).

Sikdar, S. K., and A. D. Randolph, "Secondary Nucleation of Two Fast Growth Systems in a Mixed Suspension Crystallizer: Magnesium Sulfate and Citric Acid Water Systems," *AIChE J.*, **22**, 110 (1976).

Sung, C. Y., J. Estrin, and G. R. Youngquist, "Secondary Nucleation of Magnesium Sulfate by Fluid Shear," *AIChE J.*, **19**, 957 (1973).
Van Hook, A., *Principles of Sugar Technology*, Elsevier, Amsterdam (1959).
Wey, J. S., and J. P. Terwilliger, "Effect of Temperature on Suspension Crystallization Processes," *Chem. Eng. Comm.*, **4**, 297 (1980).
Wojciechowski, B., "Structure of Water and Saturated Aqueous Solutions According to Recent Investigations," *Industrial Crystallization '81*, S. J. Jančić and E. J. deJong, Eds., North-Holland Publ. Co., Amsterdam (1982).

Manuscript received June 10, 1983; revision received January 5, 1984, and accepted January 16.

Vacancy Solution Theory of Adsorption Using Flory-Huggins Activity Coefficient Equations

New equations for the physical adsorption of gases on solids have been developed based on the vacancy solution model of adsorption in conjunction with the Flory-Huggins activity coefficient equations. The isotherm equation contains three regression parameters: a Henry's law constant, the limiting amount of adsorption, and a gas-solid interaction term. Pure-gas data over a range of temperature can be correlated using only five parameters. Gas-mixture equilibria can be predicted using only the parameters obtained from the pure-gas data. Pure-component, binary, and ternary adsorption equilibrium data on activated carbons, silica, and zeolites over a wide range of conditions have been used to evaluate the model. The results show that, except for a few systems, this model predicts gas-mixture equilibria better than any other model.

T. W. COCHRAN, R. L. KABEL and R. P. DANNER

Department of Chemical Engineering
The Pennsylvania State University
University Park, PA 16802

SCOPE

In order to exploit the physical adsorption of gases in separation processes, quantitative characterization of the multicomponent adsorption equilibria are needed as functions of temperature and pressure. Experimental multicomponent adsorption data are difficult and time-consuming to obtain; therefore, a reliable method of predicting multicomponent equilibria at various temperatures and pressures from pure-component adsorption data, and if necessary binary mixture data, would be preferred. Suwanayuen and Danner (1980a, b) proposed a vacancy solution model using the Wilson model for the activity coefficients. Although this approach has been successful for the prediction of isothermal multicomponent equilibria from single-gas isotherms alone, it fails to explicitly include the effect of temperature. Also, the equations in the Suwanayuen and Danner (S&D) model are complex, and it is often difficult to obtain physically significant parameters from the regression of limited isothermal data sets.

The objective of this work was to develop a new gas adsorption model based on vacancy solution theory which corrects the deficiencies inherent in the S&D model and surpasses it in accuracy. Any new model should account for nonideal behavior in the adsorbed phase including the adsorbate-adsorbate interactions and should predict the temperature dependency of the equilibria as well as the pressure and compositional dependencies. The model should be flexible enough to allow the use of binary data to characterize the adsorbate-adsorbate interactions if such data are available and if such binary parameters are needed. Preferably the model should include a method of estimating these adsorbate-adsorbate parameters, thus eliminating the need for the binary data which are seldom available and difficult to obtain experimentally. The model presented in this paper meets these criteria.

CONCLUSIONS AND SIGNIFICANCE

A new model for pure- and multicomponent gas adsorption is developed based on the vacancy solution theory as presented by Suwanayuen and Danner (1980a, b). Activity coefficients based on a Flory-Huggins type expression have been introduced to account for the nonideality in the adsorbed phase. By regressing five temperature-independent parameters for each component from isotherms at various temperatures, multicomponent adsorption equilibria can be predicted over an extended temperature range. The method incorporates a means of estimating the adsorbate-adsorbate interaction parameters using only pure-gas data. In most cases use of estimated parameters gives binary predictions which are just as good as using parameters extracted from the binary data.

The new Flory-Huggins based, pure-component adsorption model accurately correlated with temperature the adsorption equilibria of H_2, CO, CO_2, and light hydrocarbons on three types